Optical near-field distributions of surface plasmon waveguide modes

Jean-Claude Weeber, Yvon Lacroute, and Alain Dereux
Laboratoire de Physique de l'Université de Bourgogne (UMR CNRS 5027), 9 Avenue Alain Savary, F-21078 Dijon, France
(Received 7 January 2003; revised manuscript received 23 June 2003; published 5 September 2003)

Thin gold stripes, featuring various widths in the micrometer range, were microfabricated to obtain surface-plasmon guides on a glass substrate. Each metal stripe (MS) was excited by an incident surface-plasmon polariton which was itself launched on an extended thin gold film by the total internal reflection of a focused beam coming through the substrate. The optical near-field distributions of the surface-plasmon (sp) modes sustained by the stripes were then recorded using a photon scanning tunneling microscope (PSTM). For a fixed frequency of the incident light, these field distributions are found to depend on the widths of the stripes. We first provide an experimental study of the various order modes which arise as a function of the decreasing width. Specifically, we show that the lateral confinement of a MS surface-plasmon mode is not related to a reflection of the SP on the edges of the stripe. On the basis of PSTM images recorded over a gold thin-film step discontinuity, we show that the metal stripe plasmon modes are hybrid modes created by the coupling of interface and boundary modes. Using MSs of various thicknesses, we finally demonstrate that, similarly to the symmetric mode of an extended metal thin film bounded by different dielectric media, the field of the MS modes is mostly localized at the interface between the metal and the dielectric medium with the lowest refractive index.

DOI: 10.1103/PhysRevB.68.115401 PACS number(s): 73.20.Mf, 07.79.Fc, 78.66.−w, 42.79.Gn

I. INTRODUCTION

At optical frequencies, a surface plasmon (SP) is an electromagnetic mode which results from the oscillation of polarization charges at the interface between a metal and a dielectric medium.[1] SP modes are said to be bound to the metal surface, or to be nonradiative, when they display an evanescent decay in the dielectric medium. The conditions of excitations of SPs are well known on an extended thin film. By "extended thin film," we mean a film of finite thickness in the direction z, whose dimensions in the x and y directions are so large that they can be considered as infinite when compared with the incident wavelength. On the contrary, only few data exist about SP modes sustained by thin metal stripes (MSs) featuring micrometer widths in, for instance, the x direction. Recent works indicated that MSs can be used as surface-plasmon guides. When buried in a homogeneous dielectric medium, theoretical estimates expect that MSs can guide so-called "long-range" SP modes[2,3] over several millimeters at telecommunication frequencies.[4] For a MS deposited on a dielectric substrate, the SP mode field is more confined in the metal, leading to typical propagation lengths of a few tenths of micrometers.[5] Thus, depending on their environment, MSs could be of practical interest for building plasmonic devices useful to integrated optics[6] or for better controlled optical addressing of molecular structures. An appealing feature of the integration of MSs in reduced scale optical devices is that MSs allow the transport of both optical and electrical signals.

Mapping the intensity distribution of SP modes is necessary to fully characterize MS guiding properties. Specifically, such a mapping is essential to optimize the coupling between MSs of various widths or between the MS and other kinds of waveguides. Since the SP field decays exponentially in the direction perpendicular to the interface to which it is bounded, the observation of SP modes is conveniently achieved by a near-field optical microscope frustrating the evanescent waves. To map the electric-field intensity distribution of MS surface-plasmon modes, we used a photon scanning tunneling microscope (PSTM).[7,8] We report here on the experimental observation of fine transverse modal structures in the intensity distribution of a SP sustained by gold MSs of various widths. The PSTM was already operated to demonstrate the propagation of plasmon modes along a silver MS lying on a glass substrate,[9] but, in this previous study, the silver samples were not suitable to observe this feature of the transverse intensity profile.

II. EXPERIMENTAL SETUP

A detailed description of the PSTM setup can be found in Ref. 8. A tapered optical fiber coated with a thin layer of chromium is attached to a piezotube which enables to scan the tip over the sample within a range of a few tens of micrometers. The evanescent field frustrated by the probe propagates through the fiber to reach a photomultiplier tube. In this work, the PSTM images were obtained by scanning the probe at a constant height over the sample. Scanning the PSTM tip at a constant height without any force feedback control requires a fine adjustment of the parallelism between the scanning plane and the surface of the sample. In our setup, three micrometric screws are used to tilt the sample surface with respect to the scanning plane. With such a system, a tilt smaller than 0.06° along two perpendicular scanning axes can be routinely achieved by means of atomic force microscope (AFM) measurements. A standard AFM was also operated to obtain the topographic images shown in the following such that the PSTM and the AFM images pertaining to a same sample were not recorded simultaneously.

The samples appear in Fig. 1. They are produced by a

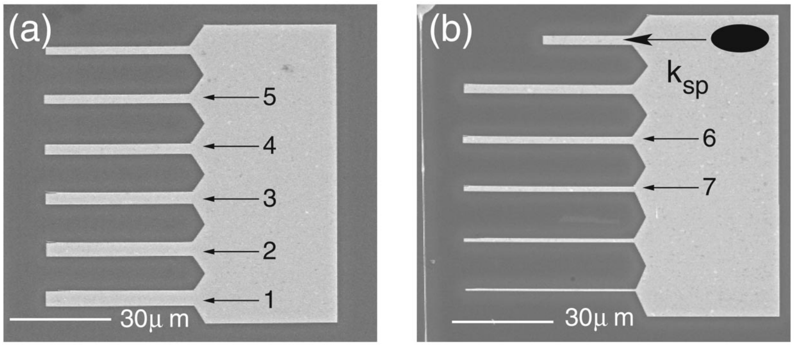

FIG. 1. Scanning electron microscope images of 55-nm-thick gold stripes. The widths of the stripes, labeled from 1 to 7, ranges from 4.5 to 1.5 μm by steps of 0.5 μm. A focused laser beam ($\lambda = 800$ nm) is incident from the substrate at an angle suitable to excite the SP on the extended thin film. An example of the location of the resulting spot is schematically shown in the upper part of (b).

microfabrication process involving the following steps: (i) electron-beam lithography on an indium-tin-oxyde–doped glass substrate spin coated with polymethyl-metacrylate (PMMA), (ii) thermal evaporation of a gold film, and (iii) lift off of the PMMA. The resulting samples are gold structures with thickness 55 ± 2 nm (roughness of 0.7-nm rms) directly deposited on the dielectric substrate. The width of the MSs ranges from 4.5 to 1.5 μm by steps of 0.5 μm. The MSs are attached to an extended thin-film area of about 35×90 μm^2. The glass substrate is optically connected with an immersion oil to a right-angle glass prism. Coming out a titanium-sapphire laser with a wavelength in vacuum $\lambda = 800$ nm, a TM polarized light beam is focused through the prism and the substrate on the extended thin-film area using a 0.15 numerical aperture lens (spot diameter at half maximum$=8.6$ μm at the focus). Adjusting the angle of incidence to about 43°, a surface-plasmon polariton is launched on the extended thin film.[9,10] As schematically shown in Fig. 1(b), two conditions are necessary for the SP launched on the extended thin film to couple efficiently with the MS plasmon modes.[9] First, the incident spot should be located in front of the MS. At the used frequency, the $1/e^2$ damping distance of a gold-air SP intensity is larger than 40 μm.[5] Therefore, even if the incident spot is located close to the right edge of the thin-film area, the SP reaches the stripes with a significant amplitude. Second, the plane of incidence must be aligned with the longitudinal axis of the MSs.

III. INTENSITY DISTRIBUTION OF METAL STRIPE SP MODES

Figure 2 shows the AFM and the PSTM images of two MS, respectively labeled 3 and 4 in Fig. 1(a) (respective width: 3.5 and 2.5 μm). The PSTM images have been obtained as the MSs were excited by the extended thin-film SP according to the procedure described above. For both stripes, the propagation of the MS mode occurs from the top to the bottom of the images. The PSTM image of the first MS [width $w = 3.5$ μm, Fig. 2(b)] has been recorded over its output end. The scattering of the incident SP mode at the edge of the stripe termination leads to an intense diffusion spot. Note that to reach the MS end, the SP mode has traveled more than 45 μm. The interference between the incident and the back-reflected plasmon mode creates a stationary wave pattern. Thanks to the weak contrast of the interference fringes, one can see three dark lines parallel to the long axis of the MSs. These longitudinal lines of the MS plasmon mode are better observed on the PSTM image recorded over the central part of the 2.5-μm-wide stripe [Fig. 2(d)]. In this case, only two dark lines appear along the MSs. In order to study the dependence of this SP modal structure as a function the MS width, a PSTM image of each stripe shown in Fig. 1 has been recorded. The transverse cross cuts (along the x axis) of these near-field optical images are displayed in Fig. 3. The MS topographic profiles obtained by the AFM (dashed lines in Fig. 3) are superimposed on these cross cuts. Since the optical and the topographic images were not recorded simultaneously, the relative position of the optical and topographic profiles have been adjusted in order to center the optical response with respect to the topography. Except for $w = 1.5$ μm, a striking feature is the strong lateral confinement of the MS surface-plasmon modes within the width of the stripe.[9] With dielectric waveguides, such a lateral confinement is obtainable only for high values of the index of refraction contrast between the core and the cladding.[11] The optical profile obtained for $w = 4.5$ μm shows only shoulders with an amplitude too small to allow an accurate measurement of their interdistance. On the contrary, four neat peaks are visible in the optical response of the MS with $w = 4.0$ μm and $w = 3.5$ μm. However, the distance p between these peaks is found to be smaller for $w = 4.0$ μm than for $w = 3.5$ μm. The two shoulders, marked by the two black arrows in Fig. 3, suggest that the optical profile of $w = 4.0$ μm does not exhibit four but six peaks. For $w = 3.0$ μm and $w = 2.5$ μm stripes, we found a profile featuring three peaks with p, respectively, equal to 580 nm and 480 nm. If the width is reduced to $w = 2.0$ μm, only two peaks arise. Finally, the optical response shows a large central peak flanked by two small amplitude oscillations located close to the edges of the stripe for $w = 1.5$ μm.

To explain the structure of the MS near-field optical response, one could first invoke a standing-wave pattern originating from the interference of the SP propagating at the stripe surface along symmetric zigzag paths (Fig. 4). If k^{MS} denotes the wave vector of the SP propagating along the stripe, the components k_x^{MS} and k_y^{MS} are, respectively, given by $k_x^{MS} = k^{MS} \cos\delta$ and $k_y^{MS} = k^{MS} \sin\delta$, where δ stands for the angle of incidence of the SP on the edges of the stripe. The component k_x^{MS} can also be written as $k_x^{MS} = \pi/p$ if p denotes the period of the interferences observed in the optical profiles. Because the excitation of the stripes is achieved

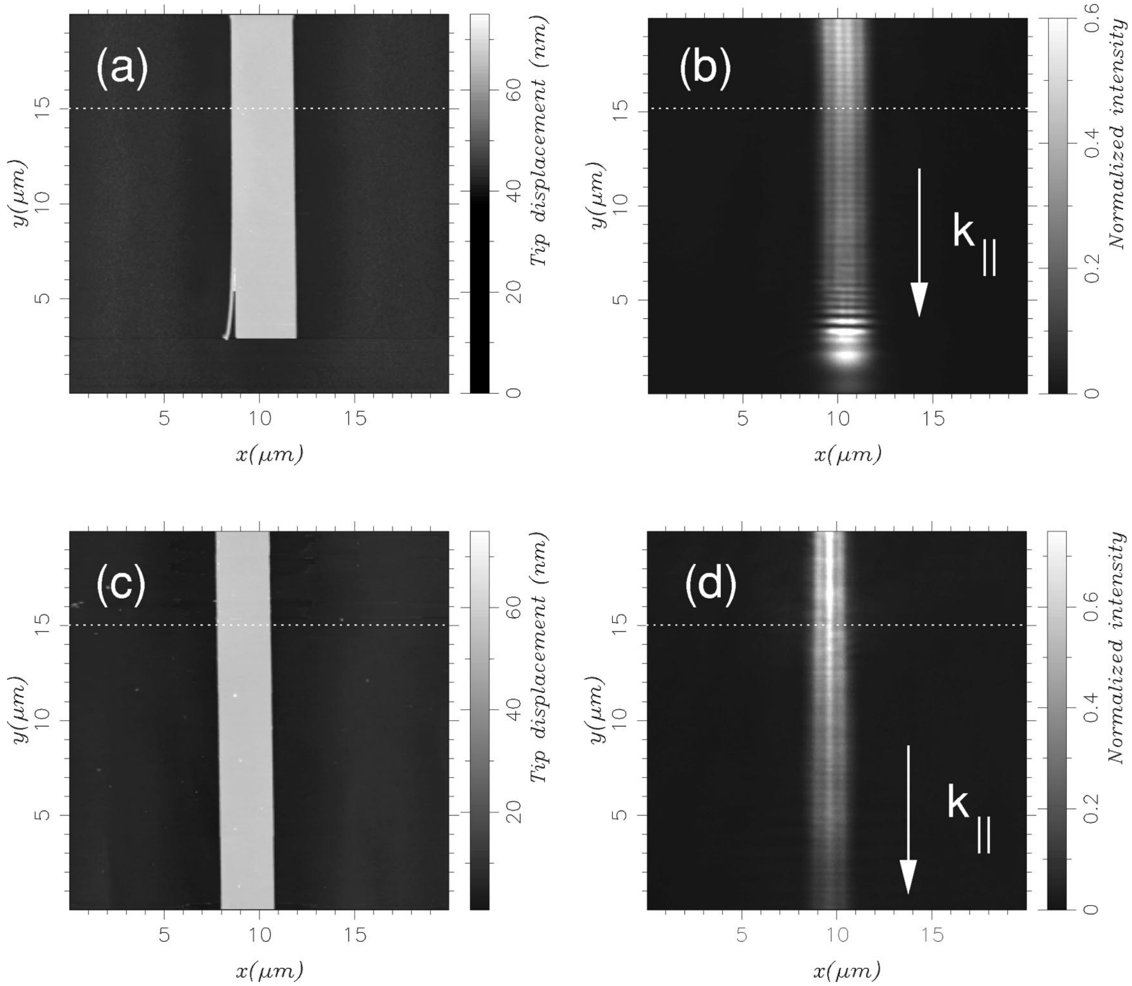

FIG. 2. [(a) and (c)] AFM and [(b) and (d)] PSTM images of two stripes: $w=3.5$ μm in (a) and (b) while $w=2.5$ μm in (c) and (d). The intensity scales of the PSTM images are normalized independently of each other: for each sample, the unit intensity is defined as the highest intensity detected above the stripe. For the sake of better visualization, the scale has been saturated to 0.6 in (b) and to 0.75 in (d).

using a surface plasmon launched on the thin-film area, we can assume that $k_y^{MS}=k_{SP}$ where k_{SP} is the wave vector of the SP propagating at the surface of a thin film. With this assumption, the angle δ is given by

$$\delta=\arctan\frac{p\times k_{SP}}{\pi}. \qquad (1)$$

The angle of incidence θ_{SP} allowing the excitation of the metal thin-film SP is given by the minimum reflection of a TM polarized collimated beam illuminating a metal thin film in the Kretschmann-Raether configuration. The metal thin-film SP wave vector can be computed from $k_{SP}=nk_0\sin\theta_{SP}$ where nk_0 is the wave vector of the incident light in the substrate supporting the thin film. For a frequency corresponding to a wavelength in vacuum of 800 nm and a gold film with a thickness of 52 nm, we found the experimental value of k_{SP} to be 7.90 μm^{-1}. From this value and the values of the periodicity p measured over the various stripes, we obtain an angle δ ranging from 47° to 55°. Then, if we suppose that the SP propagation along a stripe relies on reflections at edges, it's a simple matter to show that, for the stripes we consider, the SP should undergo several tens of reflections in order to propagate a few tens of microns. Even if a step discontinuity can reflect efficiently a surface plasmon, previous works established that the reflection of the SP on an abrupt edge of a thin film is far from being total.[12–15] Thus, such a kind of propagation would obviously lead to a dramatic damping of the SP amplitude along the stripe axis. Since we find experimentally that the damping of a MS plasmon mode is comparable to those of a SP launched on an extended thin film, we conclude that SP guiding along the MS does not rely on reflections at the MS edges. In other words, the near-field intensity distributions shown in Fig. 3 are not standing-wave patterns as in dielectric waveguides, but a genuine property of the MS surface-plasmon modes.

In order to gain more insight in the role played by the edges of the stripes, we consider the sample shown in Fig. 5(a). The sample is a rectangular gold thin-film area (thickness$=$50 nm) with a surface of 90×40 μm^2. The PSTM image of Fig. 5(b) has been recorded when the upper right corner of the thin-film area is illuminated by the incident spot. The average angle of incidence of the focused

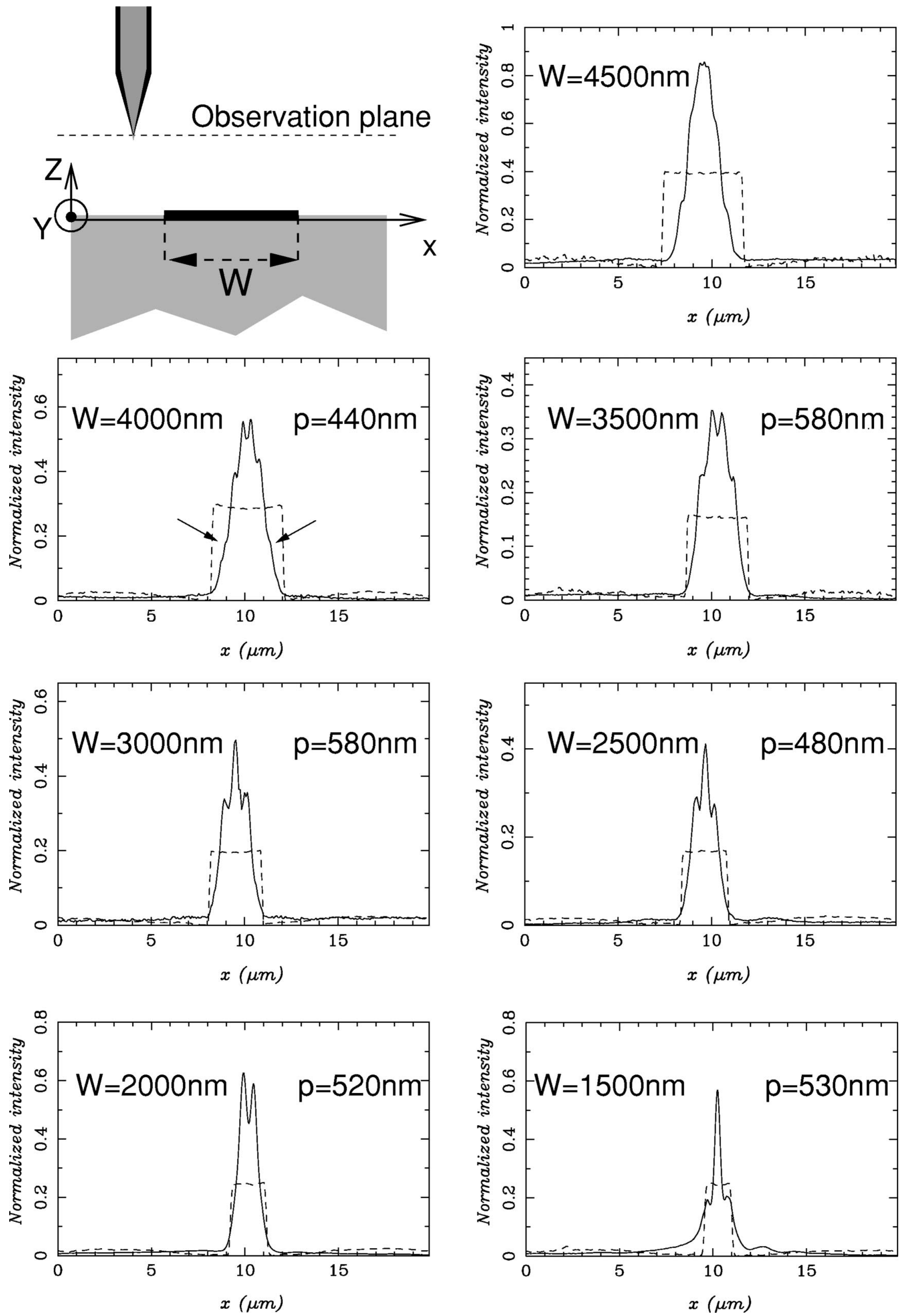

FIG. 3. Over the various stripes, cross cuts of the near-field intensity distribution recorded at a constant height. The dashed lines are guides to the eye, indicating the stripe widths (see text). The values of p give the distances between the peaks.

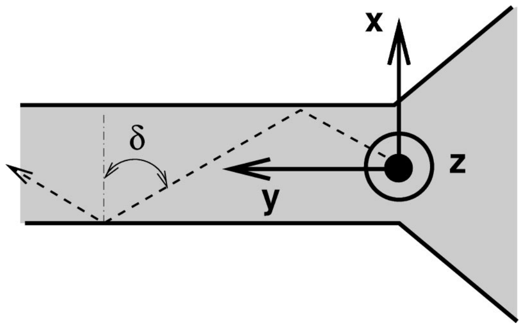

FIG. 4. Schematic view of a SP multireflection on the edges of a metal stripe.

beam was taken equal to θ_{SP} and the plane of incidence was adjusted to be parallel to the *y* axis. With these illumination conditions, a surface plasmon is locally excited on the upper part of the thin film and propagates towards the negatives values of *y*. As in the case of the stripes, we observe in the PSTM image a series of longitudinal oscillations (parallel to the *y* axis) with a period $p=480$ nm. These oscillations are even more clearly visible in the cross-cut displays in Fig. 5(d). The same kind of features is observed if the focused beam is replaced by a collimated one [Fig. 5(c)]. In this case, the plasmon is excited over the whole surface of the thin film. The interference of the incident SP and the SP back reflected by the edge of the thin film perpendicular to the plane of incidence leads to a standing surface-wave pattern parallel to the *x* axis. For an incident SP with a positive *x* wave-vector component, a reflection on the thin-film edge parallel to the *y* axis could also explain the longitudinal oscillations parallel to the *y* axis. However, as in the case of the MS, the angle of incidence δ of the SP on the edge should be around 50° in order to create a standing-wave pattern with a period of 480 nm. Since the plane of incidence was adjusted to be parallel to the *y* axis, such an angle of incidence δ is unrealistic. In addition, one can see in Fig. 5(c) that the amplitude of the longitudinal oscillations parallel to the *y* axis is damped over a typical distance of about 2 μm while no damping is visible for the standing-wave pattern parallel to the *x* axis. On the basis of these observations, we suggest that the longitudinal oscillations parallel to the *y* axis probably

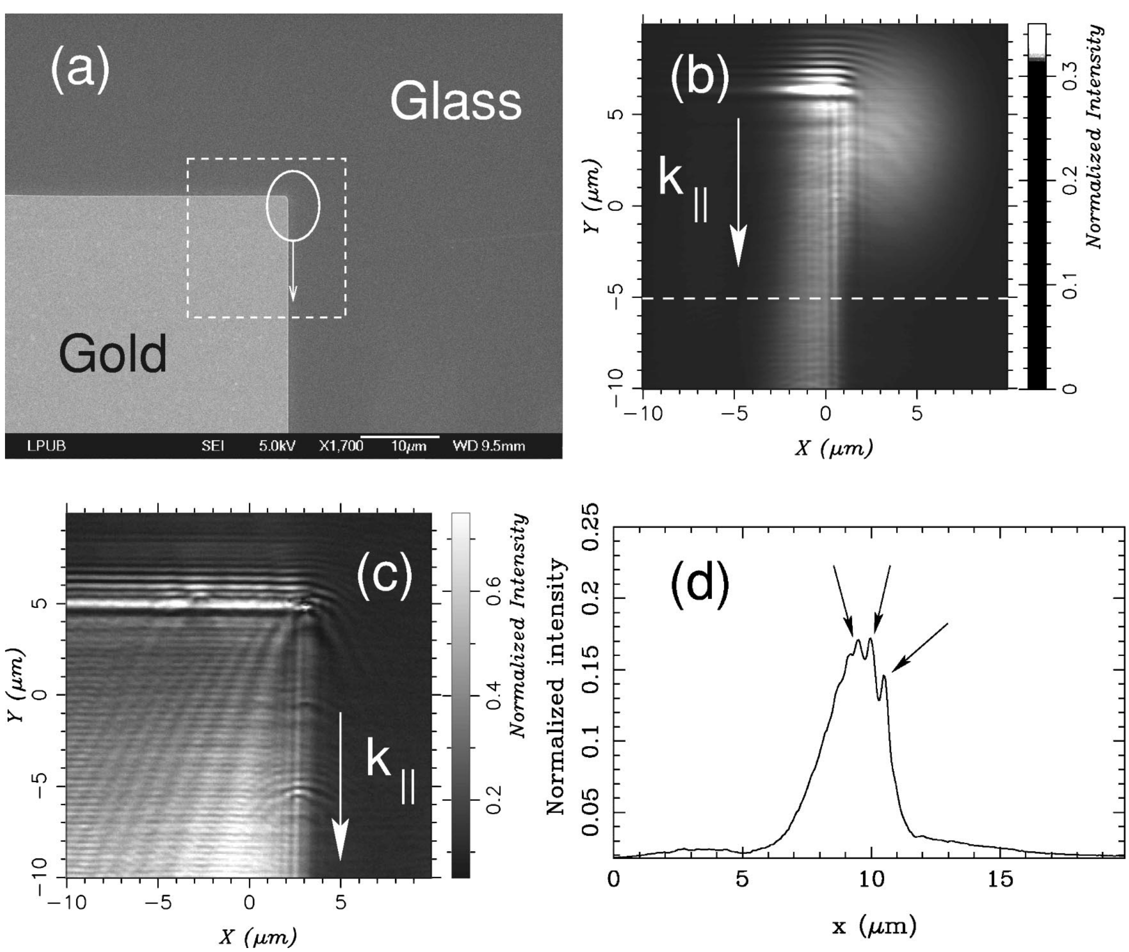

FIG. 5. (a) Scanning electron microscope (SEM) image of a step discontinuity of a gold thin film. (b) PSTM image recorded over the surface defined by the white dashed perimeter drawn in (a). The upper right corner of the gold thin-film area is excited by an incident focused spot. The location of the incident spot is schematically shown in (a). The plane of incidence is parallel to the *y* axis. (c) Same as (b) except that the incident beam is not focused anymore but collimated (spot diameter 600 μm). A surface plasmon is excited over the whole surface of the gold thin film. (d) Cross cut of the image (b) taken along the white dashed line.

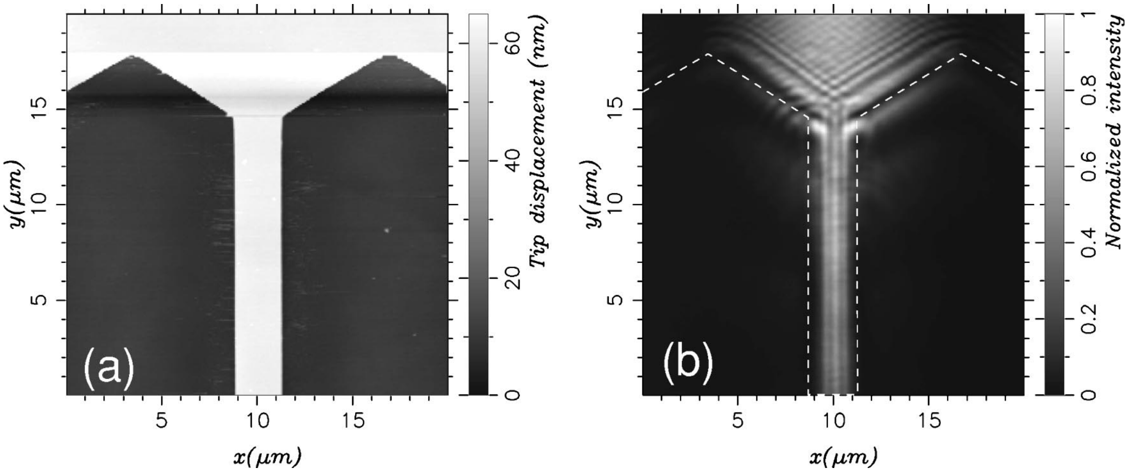

FIG. 6. (a) AFM and (b) PSTM images of the junction between the extended thin film and the 2.5-μm-wide stripe.

correspond to the near-field distribution of a mode supported by a boundary between a semi-infinite metal thin film and a dielectric medium. Recent numerical results[2,16] demonstrate that highly confined edge modes (called ''corner modes'' in Refs. 2 and 16) are expected at the step discontinuity of a metal thin film and a dielectric medium. However, both the confinement and the field enhancement of these type of modes are very sensitive to the geometry of the edge.[17] Probably because the lithographic technique does not allow to achieve edges with a radius of curvature smaller than a few tens of nanometers, we do not observe genuine edge modes but rather SP modes that characterize the presence of the thin-film boundary. Note that similar types of oscillating ''boundary modes'' with a degree of localization lower than that of the edge modes have been described in the context of surface phonons at the transverse boundary between two semiconducting media.[18] From the results obtained for the extended thin-film boundary, one can now suggest that the stripe modes might be hybrid modes resulting from the coupling of these boundary modes and the modes associated with the large upper gold-air interface defined by the constant $z=50$ nm plane. Indeed, the optical profiles of each stripe (Fig. 3) feature a Gaussian-like intensity distribution (associated with the finite width interface mode) modulated by the oscillations related to the two boundary modes supported by each lateral (constant x coordinate) boundary of the MS.

IV. MULTIMODE OR MONOMODE EXCITATION?

At this stage, due to the focused nature of the incident beam, we cannot unambiguously determine if the measured intensity distribution is due to the excitation of only one or several MS surface-plasmon modes. A definitive answer to this question is not possible in the absence of the width-dependent dispersion relations of SP modes supported by MSs bounded by different dielectric media such that a large contrast of the index refraction arises between the substrate (glass in our case) and the external medium (air in our case).[16] However, two arguments favor the thesis of the excitation of only one MS surface-plasmon mode.

First, as mentioned above, the stripes analyzed in Figs. 2 and 3 are not directly excited by the focused beam but by the SP launched on the extended thin-film area. The resonance linewidth of this launched SP that reaches the stripe imposes a narrow range of wave-vector components $k_\parallel$ which are parallel to the surface. This suggests that the SP launching process has filtered a single $k_\parallel = k_{SP}$ out of those provided by the numerical aperture of the focusing lens. In other words, the extended thin-film area acts as a narrow bandpass $k_\parallel$ filter, selecting k_{SP}. Such a technique excites only the MS surface-plasmon modes whose dispersion relation cuts the line $k_\parallel = k_{SP}$ at the incident frequency $\omega_0 = 2\pi c/\lambda$ (c being the speed of light in vacuum). The excitation of several modes would imply that the dispersion relations of the MS surface-plasmon modes display several branches in the vicinity of the point (ω_0, k_{SP}). In this case, the illumination conditions should lead to the excitation of the mode whose phase constant is the closest to k_{SP} at the incident frequency.

A second argument favoring the excitation of only one MS surface-plasmon mode relies on the invariance of the transverse-modal structure along the longitudinal axis of the stripe. Let us consider the PSTM image of the junction between the extended thin-film area and the $w=2.5$ μm MS [Fig. 6(b)]. The SP launched on the extended thin-film area is visible in the upper part of this image. The characteristic three-peak transverse profile is established above the MS in the very first few micrometers after the junction to the extended thin-film area. Note that no spatial transient is visible around this junction zone. This suggests that coupling the launched SP to the MS surface-plasmon mode does not induce any significant radiation losses.[19] One can also observe that the three-peak structure remains stable all along the stripe and is similar to those recorded further away from the junction zone in Fig. 2(d). If we assume a multimodal excitation of the MS, at a constant height z_0 above the stripe, the electric field of the SP propagating along the MS reads

$$\vec{E}(x,y,z_0) = \sum_m \vec{E}^{(m)}(x,z_0)\exp[-\alpha^{(m)} + i\beta^{(m)}]y, \quad (2)$$

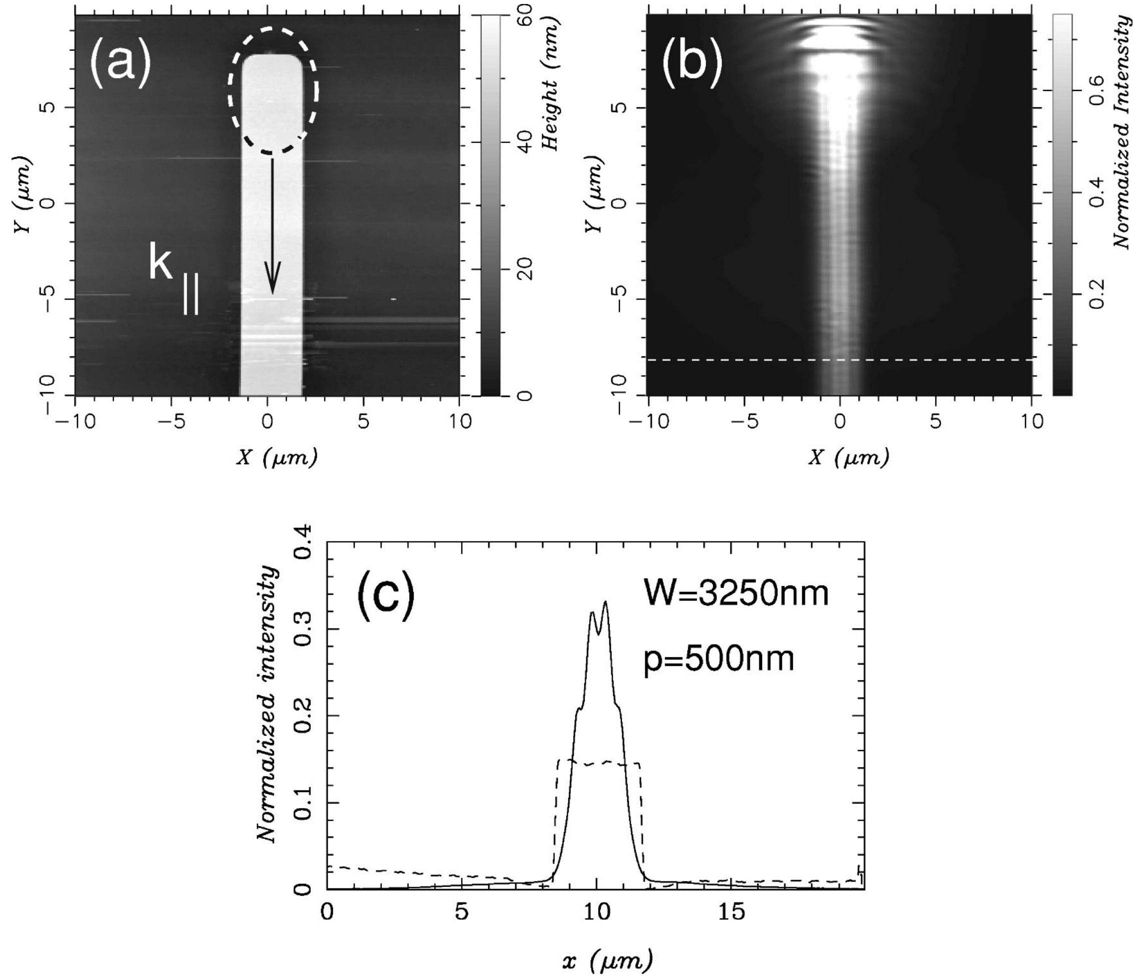

FIG. 7. (a) Topographic image of a MS with a width $W = 3.25$ μm and thickness $t = 55$ nm. (b) PSTM image recorded when the input end of the MS is directly illuminated by the incident spot. The average angle of incidence is equal to θ_{SP} and the plane of incidence is parallel to the y axis. (c) Cross cut of (b) taken along the white dashed line. The period of the longitudinal oscillations is 500 nm.

where $\vec{E}^{(m)}(x,z_0)$, $\alpha^{(m)}$, and $\beta^{(m)}$ denote, respectively, the amplitude, the attenuation constant, and the phase constant of each MS surface-plasmon mode. In the illumination conditions detailed above, the simultaneous excitation of several MS modes implies that their phase constants should be equal (or at least very close) to k_{SP}, so that the expression of the electric field becomes

$$\vec{E}(x,y,z_0) = \sum_m \vec{E}^{(m)}(x,z_0)\exp[-\alpha^{(m)} + ik_{SP}]y. \quad (3)$$

The observed invariance of the transverse profile of the near-field intensity distribution along y requires also the equality of the attenuation constants of all the modes simultaneously excited. Indeed, the relative weights of each mode involved in the above expansion of the total field must be kept constant as a function of y in order to agree with the observed invariance. Thus, it turns out that the hypothesis of a multimodal excitation implies the equality of both the phase *and* attenuation constants of all the MS surface-plasmon modes which are simultaneously excited. Since these two constants are usually not equal from one MS surface-plasmon mode to the other,[2,16] we conclude that there is a very high probability that the experimental images show the intensity distribution of only one mode for each MS.

Up to now, the metal stripes have been excited by coupling with a SP locally launched on an extended thin-film area. With the aim of checking the influence of the excitation conditions on the near-field intensity distribution, we consider now a direct illumination of a gold stripe having a width of 3.25 μm. Figure 7(a) shows a topographic image of this stripe and the location of the incident spot. The average angle of incidence of the focused beam was taken equal to θ_{SP} and the plane of incidence was adjusted to be parallel to the y axis. Both the PSTM image [Fig. 7(b)] and the optical profile displays in Fig. 7(c) show a four-peak intensity distribution in agreement with the optical response of the MS having approximately the same width ($W = 3.5$ μm in Fig. 3). Except for the period of the peaks, which is now 500 nm instead of 580 nm, the optical profiles obtained for $W = 3.5$ μm and $W = 3.25$ μm are very similar. This observation leads to the conclusion that the direct illumination of

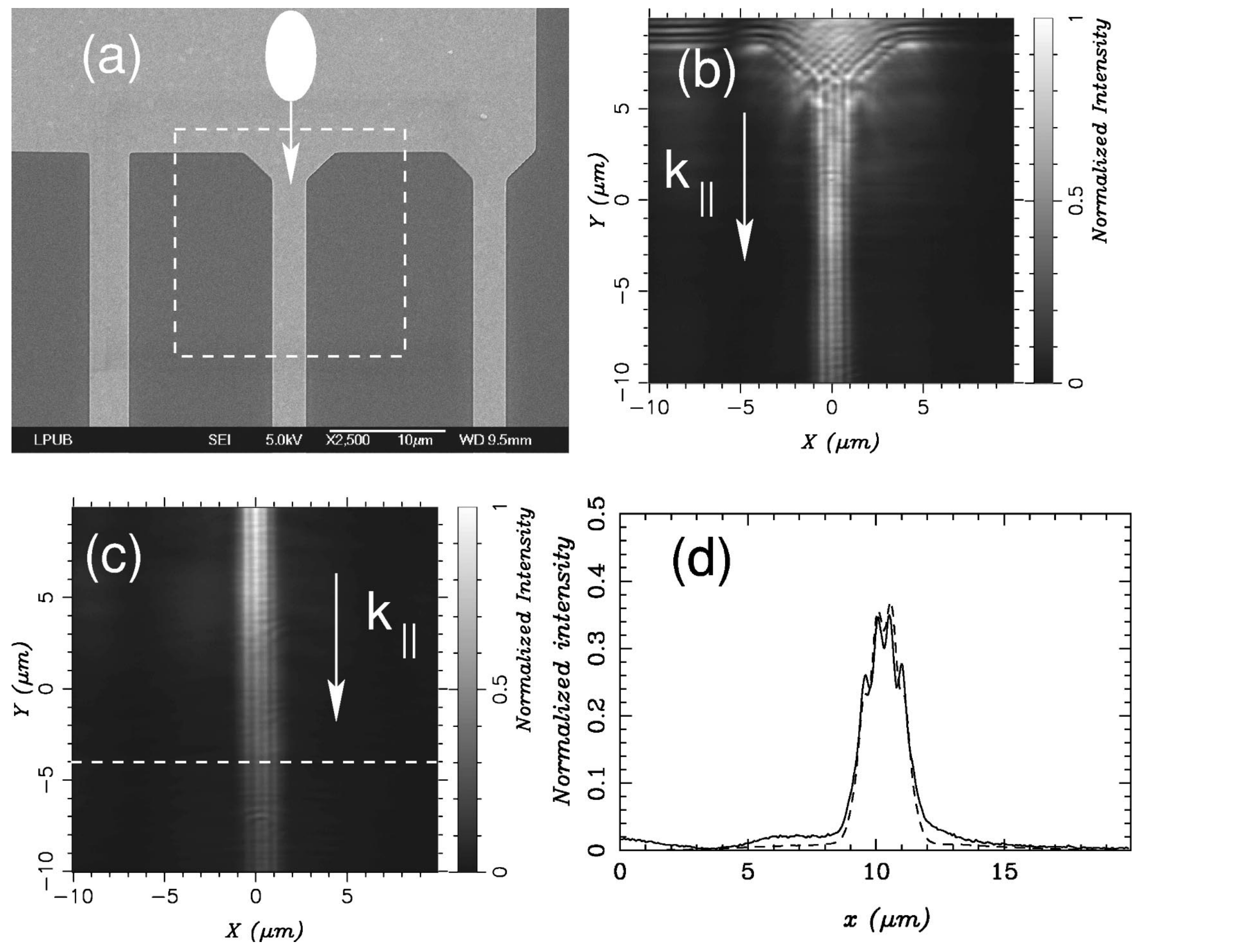

FIG. 8. (a) SEM image of the "thick" sample. (Thickness = 120 nm.) (b) PSTM image recorded over the junction zone defined by the white dashed square drawn in (a). The width of the MS is $W = 3.25$ μm. The excitation of the MS is achieved by coupling with a SP locally launched by the incident focused beam. The incident spot is localized on the extended thin-film area. (c) Same as (b) except that the image is taken after a propagation of the MS mode over more than 20 μm. (d) Solid line: Cross cut of image (c) taken along the white dashed line. Dashed line: Optical profile shown in Fig. 7(c) (thickness = 55 nm). Note that the amplitude of this profile has been adjusted for the sake of easier comparison between the optical responses of the "thick" and the "thin" MSs.

MS does not allow the excitation of SP modes different from those excited by coupling with a thin-film SP. It is worthwhile to notice that this result arises in spite of the wide range of $k_\parallel$ incident on the MS when it is directly illuminated by the focused beam. It turns out that even if the dispersion curve of several MS modes cuts the line $\omega = \omega_0$ in the range of $k_\parallel$ defined by the angular width of the incident beam, only one mode is efficiently excited with this type of illumination. Since these arguments all lead to the conclusion that the observed field distributions are related to a single mode excitation, we now discuss in detail the characteristics of this mode in the next section.

V. INSIGHT INTO THE DISPERSION RELATIONS OF A METAL STRIPE SP

The numerical results of Ref. 16 demonstrate that the coupling between SP modes supported, respectively, by the substrate/metal and metal/superstrate interfaces can make the field distribution of MS modes very sensitive to the thickness of the metal film. This property is true for a symmetric MS [optical indices of the substrate (n_{sub}) and superstrate (n_{sup}) are equal] but also for an asymmetric system ($n_{sub} \neq n_{sup}$) even in the case of large asymmetry. In order to check the behavior of the MS modes with respect to the thickness of the metal film, the sample shown in Fig. 8(a) was fabricated: a MS with a width of 3.25 μm connected to a large thin-film area. The main difference between this sample and the previous ones is the thickness of the gold film measured to be 120 nm by atomic force microscopy. We found experimentally this thickness to be the largest that allows the excitation of a surface plasmon at the gold/air interface of the thin film in the Kretschmann-Raether configuration using our focused beam. Figure 8(b) shows the PSTM image recorded over the junction area defined by the white dashed square drawn in Fig. 8(a). A four-peak structure is visible over the stripe. The structure can be observed even after a propagation of more than 20 μm [Fig. 8(c)]. The optical profiles obtained for the "thick" MS and the "thin" MS previously studied in Fig. 7

are superimposed in Fig. 8(d) after normalizing the maxima of each profile to a common value. Note that, because the field enhancement of a SP excited at the surface of a "thick" film is in absolute value lower than that for a "thin" film,[1] this normalization procedure gives the impression that the profile of the "thick" MS [solid line in Fig. 8(d)] exhibits a weaker confinement along the x axis than that of the profile of the "thin" MS [dashed line in Fig. 8(d)]. Because the two profiles are qualitatively similar, we conclude that the thickness of the film does not play a key role in the field distribution of the MS plasmon modes. Thus, the modes we observe are not created by a coupling of SPs supported by the upper and lower interfaces of the MS.

When excited by coupling with a SP launched on the thin-film area, the electromagnetic field incident on a MS is mostly localized at the upper (metal/air) interface. The main component of the electric field associated with a thin-film SP is known to be the component perpendicular to the substrate surface (z direction in our case, see Fig. 4). If the thin-film SP propagates along the y axis, the z component of its electric field is then symmetric with respect to the yz plane. Thus, according to the nomenclature defined in Ref. 16, such a field should allow an efficient excitation of a "SS_b^n"-type MS mode, where n labels the number of extrema along the x axis of the MS mode electric-field z component. As we mentioned previously, the cross sections of the MSs we consider are not perfectly rectangular such that it is difficult to push further the analysis of our experimental results by direct comparison with the numerical computations of Ref. 16. In particular, the number of peaks we observe in the optical profiles of the MS modes cannot be interpret as the value of n previously defined. Nevertheless, one can get some insight in the width-dependent dispersion relation of the MS plasmon modes from our experimental observations.

The near-field optical profiles (Fig. 3) show that, for a fixed frequency, decreasing the MS width may have two main consequences on the SP mode intensity distribution. First, the distance between the peaks can be reduced while the number of peaks is kept constant such as, for example, in the transition from $w=3.0$ μm to $w=2.5$ μm. Second, if the width is further reduced below a critical width, the number of peaks is lowered, as, for example, in the transition from $w=3.5$ μm to $w=3.0$ μm or that from $w=2.5$ μm to $w=2.0$ μm. Both behaviors suggest that, at the frequency ω_0, a mode featuring a given number of peaks may occur in some range of widths. Below some critical width, the dispersion curve of a given mode (with a characteristic number of peaks) probably shifts toward higher energy such that it is not possible anymore to excite it at the said frequency ω_0. Thus, below this critical width, the number of peaks in the MS plasmon mode profile is lowered.

This reasoning seems to be refuted by the transition from $w=2.0$ μm to $w=1.5$ μm. In this case, the number of peaks in the transverse modal profile increases from two to three. However, in the near-field optical transverse profile of the 1.5-μm-wide stripe, the amplitude of the central peak is much larger than those of the two other peaks which are located very close to the edges of the stripe. This localization suggests that such peaks might be related to the strong coupling of the two boundary modes. This assumption is difficult to verify at this stage but would at least restore the consistency of the reduction of the number of peaks associated with the transverse profile of the SP mode when decreasing the width of the MS. Contrasting with the SP modes confined within the width of the stripes observed for $w>1.5$ μm, the intensity decaying far away outside the stripe provides another striking feature of this width $w=1.5$ μm. In analogy with dielectric waveguides, this somewhat softer confinement could indicate that 1.5 μm is close to the "cutoff width" of this mode.

VI. CONCLUSION

In summary, we have used a PSTM to observe the near-field intensity distribution of plasmon modes propagating on gold stripes featuring widths in the micrometer range. The illumination conditions allowed to excite the stripes by coupling with a surface-plasmon polariton launched on an extended thin-film area. For a fixed frequency corresponding to a wavelength in vacuum of 800 nm, the PSTM images show that the MS surface-plasmon modes remain well confined within the stripe widths. If the MS width is not too large, the near-field optical transverse profiles of the MS surface-plasmon modes exhibit an intensity distribution showing periodic oscillations along the transverse axis. By comparing the field distribution observed over a MS excited either by direct illumination with the incident focused spot or by coupling with a SP launched on an extended thin film, we conclude that the features of the MS optical profiles are probably related to the excitation of a single MS mode. From the PSTM observation of a single metal thin-film step discontinuity, we show that the transverse features in the field distribution of the MS plasmon mode are related to modes pertaining to an abrupt boundary between a metal thin film and a dielectric medium. These observations lead to the conclusion that the propagation of SP modes along MSs does not rely on reflections on the lateral edges of the metal stripe. Thus, the propagation of a SP along a MS is fundamentally different from the propagation of guided modes in standard dielectric waveguides. One can then anticipate specific guiding properties of MSs. The similarity of the intensity distributions recorded over MSs having the same width but different thickness demonstrates that the field of the MS modes is mostly localized at the upper interface (metal/air). Even if the frequency dependence of the metal dielectric function prevents a straightforward extrapolation of the MS optical properties to other frequencies, the experimental results reported here, at a fixed frequency and for different widths, provide a useful insight into the dispersion relations of MS surface plasmons.

ACKNOWLEDGMENTS

This work was supported by the Regional Council of Burgundy (ARCEN project) and by the French CNRS (STIC: Grant No. EPML 20).

[1] H. Raether, *Surface Plasmons*, Springer Tracts in Modern Physics Vol. 111 (Springer, Berlin, 1988).
[2] P. Berini, Phys. Rev. B **61**, 10 484 (2000).
[3] P. Berini, Opt. Express **7**, 329 (2000).
[4] R. Charbonneau, P. Berini, E. Berolo, and E. Lisicka-Shrzek, Opt. Lett. **25**, 844 (2000).
[5] B. Lamprecht, J.R. Krenn, G. Schider, H. Ditlbacher, M. Salaerno, N. Feldidj, A. Leitner, and F.R. Aussenegg, Appl. Phys. Lett. **79**, 51 (2001).
[6] H. Ditlbacher, J.R. Krenn, G. Schider, A. Leitner, and F.R. Aussenegg, Appl. Phys. Lett. **81**, 1762 (2002).
[7] R.C. Reddick, R.J. Warmack, and T.L. Ferrell, Phys. Rev. B **39**, 767 (1989).
[8] A. Dereux, E. Devaux, J.C. Weeber, J.P. Goudonnet, and C. Girard, J. Microsc. **202**, 320 (2001).
[9] J.C. Weeber, J.R. Krenn, A. Dereux, B. Lamprecht, Y. Lacroute, and J.P. Goudonnet, Phys. Rev. B **64**, 045411 (2001).
[10] P. Dawson, F. de Fornel, and J.P. Goudonnet, Phys. Rev. Lett. **72**, 2927 (1994).
[11] R. Quidant, J.C. Weeber, A. Dereux, D. Peyrade, G. Colas des Francs, Ch. Girard, and Y. Chen, Phys. Rev. E **64**, 066607 (2001).
[12] J.A. Sánchez-gil, Appl. Phys. Lett. **73**, 3509 (1998).
[13] R.F. Wallis, A.A. Maradudin, and G.I. Stegeman, Appl. Phys. Lett. **42**, 764 (1983).
[14] T.P. Shen, R.F. Wallis, A.A. Maradudin, and G.I. Stegeman, Appl. Opt. **23**, 607 (1984).
[15] See, for example, Figs. 3(b) and 3(c) of Ref. 8.
[16] P. Berini, Phys. Rev. B **63**, 125417 (2001).
[17] J.P. Kottmann, O.J.F. Martin, D.R. Smith, and S. Schultz, Phys. Rev. B **64**, 235402 (2001).
[18] Ph. Lambin, T. Laloyaux, A.A. Lucas, and J.P. Vigneron, Phys. Rev. B **35**, 5621 (1987).
[19] A.W. Snyder and J.D. Love, *Optical Waveguide Theory* (Chapman & Hall, London, 1983).